ELSEVIER

Ceramics International 33 (2007) 751–759

CERAMICS
INTERNATIONAL

www.elsevier.com/locate/ceramint

Effect of zircon additions on low and ultra-low cement alumina and bauxite castables

M.F. Zawrah *

National Research Center, Ceramics Department, 12622 Dokki, Cairo, Egypt

Received 6 June 2005; received in revised form 12 October 2005; accepted 4 December 2005
Available online 11 April 2006

Abstract

Two series of low- and ultra-low alumina castables were prepared from calcined Chinese bauxite and pure alumina aggregates. Both series consisted of 90 wt.% aggregate and 10 wt.% high alumina cement (HAC), with HAC replaced by 2, 4, 6 and 8 wt.% zircon to obtain castables containing an in situ mullite–zirconia composite in the matrix to improve their microstructure, physico-mechanical and refractory properties. The samples were characterized in terms of densification parameters (bulk density and apparent porosity), cold crushing strength (CCS), XRD, SEM and thermal shock resistance (TSR) to understand the effect of zircon additions on the castable composition and properties. Generally, the results revealed that castables containing bauxite aggregate showed higher densification and mechanical properties due to the presence of some impurities in the bauxite aggregate which help liquid phase sintering, and consequently, improved the mechanical properties. Castables containing pure alumina exhibited higher refractory properties due to their higher purity, i.e. the absence of a liquid phase. The emergence of refractory phases such as alumina, mullite and zirconia was observed to have beneficial effects on physico-mechanical and refractory properties due to the development of morphologies which interlocked other phases, and to pore filling from expansible reactions.

Keywords: C. Mechanical properties; D. Al_2O_3; Refractory properties; Castables

1. Introduction

A significant increase in the life of high alumina-based refractory castables has been possible by decreasing the cement content, thus avoiding liquid phase formation at working conditions, which in turn improves the corrosion resistance and creep strength [1–4]. Trends for increasing utilization of monolithic refractories over the past decade have been accompanied with the parallel trend of the replacement of calcium aluminate cement (CAC) with CAC-free bonding systems [5–7]. The reason for the replacement or reduction of CAC content in monolithic refractories can be attributed to the effect of lime on those refractory systems. Often, in the presence of lime (CaO), low melting temperature compounds may be formed, or lower melting eutectics may develop through reactions in those refractory systems. For example, in the $CaO–Al_2O_3–SiO_2$ ternary system, there are five ternary eutectics with melting points below 1350 °C [8]. These low melting temperatures are unacceptable for many metallurgical processes. One approach to the replacement of lime has been to develop or utilize CAC-free or CaO-free bonds in the refractory linings. These advances have taken several different technical approaches to develop satisfactory bonds within the refractory aggregate systems. Those approaches may be classified as: (i) the addition of a fine particle size of an oxide component that reacts with the primary oxide of the refractory to form a direct bond between the aggregate, or (ii) the addition of multiple oxides that react in an in situ manner to form a high melting point compound that serves as the direct bond between the individual grains of the refractory system.

The attractiveness of low cement and ultra-low cement bauxite castables for refractory applications is due not only to their high strength, thermal shock resistance (TSR) and corrosion resistance; but also to their economical effectiveness coming from the use of natural bauxite resources. They have already been successfully employed in molten iron torpedo cars, blast furnace troughs and incinerator linings, and may still acquire wider applications in high temperature industries [9]. In the last three decades, there was a great deal of interest in improving the quality of refractory castable through decreasing

---

* Fax: +20 2 3370931.
E-mail address: mzawrah@hotmail.com.

0272-8842/$32.00 © 2006 Elsevier Ltd and Techna Group S.r.l. All rights reserved.
doi:10.1016/j.ceramint.2005.12.019

the cement content; i.e. 4–8% in low cement castables (LCC), 1–3% in ultra low cement castables (ULCC), or <1% in zero cement castables (ZCC) [10–14]. Modern refractory castables (LCC and ULCC) are complex mixtures of calcium aluminate cement, ultra fine materials, aggregates and admixtures. These castables develop very high performance during and after heating. They are used when thermal shock resistance or resistance against abrasion and corrosion by slags or melting metals is required. These castables require good control installation, i.e. rheology and hardening kinetics, which are influenced not only by the intrinsic reactivity of the calcium aluminate cement, but also by the interactions between fillers and calcium aluminate cement [15–17].

In previous investigations [18–24], lower amounts of cement, in conjunction with fine grain sized materials having high surface area and dispersing aids, were used. Those materials were silica fume, Al_2O_3, Cr_2O_3, ZrO_2, TiO_2, SiC, clay mineral and carbon. It was concluded that the presences of such materials promote refractory properties such as volume stability and well balanced physical and hot mechanical properties. The presence of zircon with fine alumina as a filler tends to form mullite and ZrO_2 after firing. The formation of mullite and zirconia are of vital importance as these bonding phases exhibit high refractoriness, low creep rate, low thermal expansion, good chemical and thermal stability, and good toughness and strength [25,26].

This work researches the refractory properties of bauxite and alumina castables through in situ formation of mullite–zirconia composite.

2. Materials and experimental procedures

2.1. Materials

Graded calcined Chinese bauxite and pure alumina of particle size distribution 70 wt.% coarse; (2.36–0.6 mm), 5 wt.% medium; (0.60–0.25 mm), and 25 wt.% fine; (<0.25 mm) were used as starting aggregate in this investigation. A constant weight of 90 wt.% of the graded aggregate was used to prepare the castable batches together with 10 wt.% of high alumina cement (HAC Lafarge, C-80). Other compositions of castable batches were prepared by substituting 2, 4, 6 and 8 wt.% of the cement with zircon to prepare castables-containing mullite–zirconia composites as a matrix. The prepared castable samples are referred to as Z0B, Z2B, Z4B, Z6B and Z8B for castables based on bauxite aggregate and as Z0A, Z2A, Z4A, Z6A and Z8A for castables based on pure alumina. The chemical analysis of staring raw materials and the compositions of the prepared castable batches are given in Tables 1 and 2.

2.2. Preparation and characterization

The dry batches were hand mixed for 3 min at 25 °C with an adequate amount of water, which was determined for each batch according to the standard "good ball in hand" test [27]. The mixed batches were then cast into cubes of 25 mm side length in steel moulds using a vibrating table at a frequency of 50 Hz and 4 min vibrating time. The castable samples were left in their moulds for 24 h in a 100% relative humidity cabinet. The hydrated samples were then remolded and further cured for 7 days in the same cabinet at 22 °C. The hydrated samples were subsequently tested for cold crushing strength (CCS), bulk density and apparent porosity before and after firing at 1550 °C for 2 h (5°/min, heating rate), according to ASTM standard C133-91 and Egyptian standard 1859 (1990). After hydration, bulk density and apparent porosity were in the range 2.5–2.7 g/cm^3 and 20–30%, respectively. The fired castables were also characterized with respect to their solid phase composition using a Philips 1730 diffractometer with a Ni filtered Cu Kα radiation at a scan speed of $1^\circ\ min^{-1}$. A Joel XL 30 scanning electron microscope (SEM) was used to examine the microstructure of the fired samples. The refractory properties were assessed by carrying out refractoriness under load (RUL) according to ISO standard 1893 (1989), permanent linear change (PLC) according to ISO standard 2478 (1987) and thermal shock resistance according to an air quenching technique [28–31]. To evaluate the thermal shock resistance of castables, the residual strength ratio was determined after ten thermal shock cycles from 1000 °C to room temperature ($\Delta T = 1000$ °C). Also, the critical temperature difference (ΔT_c) was determined from residual strength ΔT curves from zero to 1300 °C for two specimens (Z8B and Z8A) after one thermal shock cycles.

Table 1
Chemical analysis of starting raw materials

Oxide	Chemical analysis (wt.%)			
	Bauxite	Pure alumina	HAC	Zircon
SiO_2	6.70	–	0.40	32.17
Al_2O_3	86.00	99.6	79.00	0.88
Fe_2O_3	2.62	–	0.25	0.15
TiO_2	3.72	–	–	0.15
CaO	0.12	–	20.00	–
MgO	0.09	–	0.20	–
ZrO_2	–	–	–	66.62

Table 2
Designed batch compositions (wt.%)

Number	Aggregate	HAC	Zircon
Bauxite castables			
Z0B	90	10	0
Z2B	90	8	2
Z4B	90	6	4
Z6B	90	4	6
Z8B	90	2	8
Alumina castables			
Z0A	90	10	0
Z2A	90	8	2
Z4A	90	6	4
Z6A	90	4	6
Z8A	90	2	8

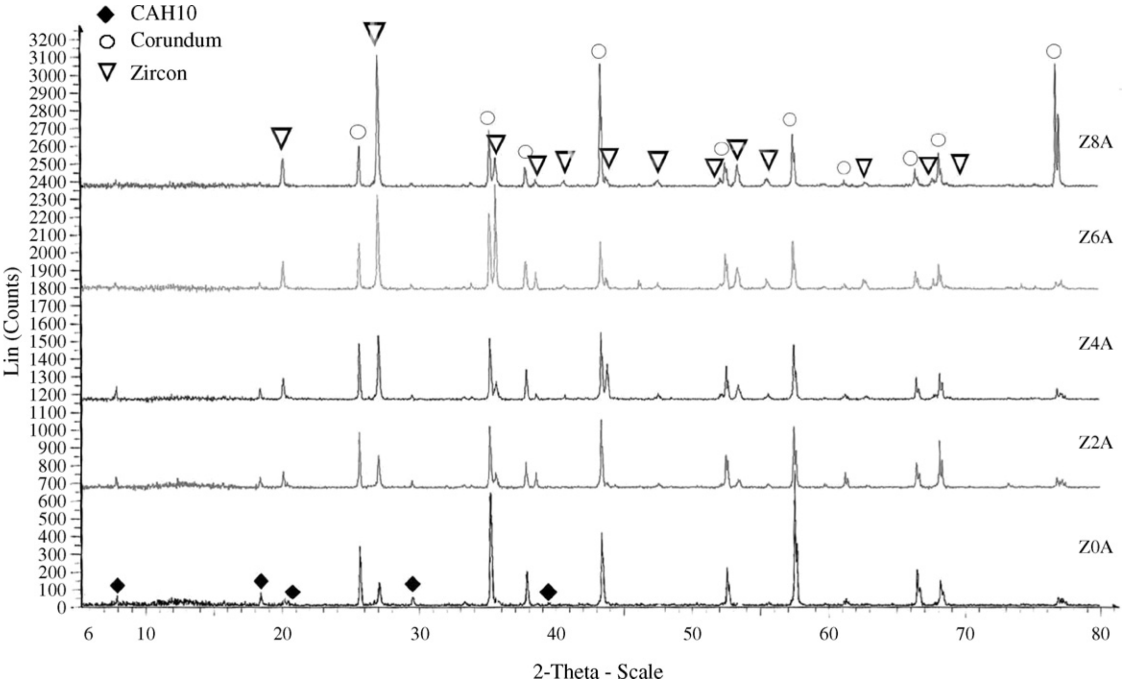

Fig. 1. XRD of hydrated alumina castables.

3. Results and discussion

3.1. Phase composition

Fig. 1 shows X-ray diffraction pattern (XRD) of the green (20 °C) castable samples prepared from pure calcined alumina aggregate after curing in air for 7 days at ambient temperature. From Fig. 1, we see that the control castable (i.e. zero zircon-containing castable) consists mainly of alumina and calcium aluminate hydrate (CAH_{10}) phases. The hydrated phase is produced from the hydration of the added high alumina cement after curing in a relative humidity of 100% for 7 days. As we proceed from the Z0A to Z8A castable samples, CAH_{10} phase decreases and a new zircon phase increases. A corundum phase (α-Al_2O_3) was present in all samples as expected.

On the other hand, the investigated castable samples prepared from pure Chinese bauxite and calcined alumina fired at 1550 °C are shown in Figs. 2 and 3. It appears that the control castable sample [free from zircon (Z0B and Z0A)] composed mainly of corundum with some peak lines characterizing CA, in the case of bauxite castables, and CA_6 minerals, in the case of alumina castables. CA results from the polymorphous conversion of calcium aluminate hydrate products to the original phases CA. The formation of CA_6 in alumina castables is attributed to the higher alumina content of starting alumina aggregate. In both castable series (calcined

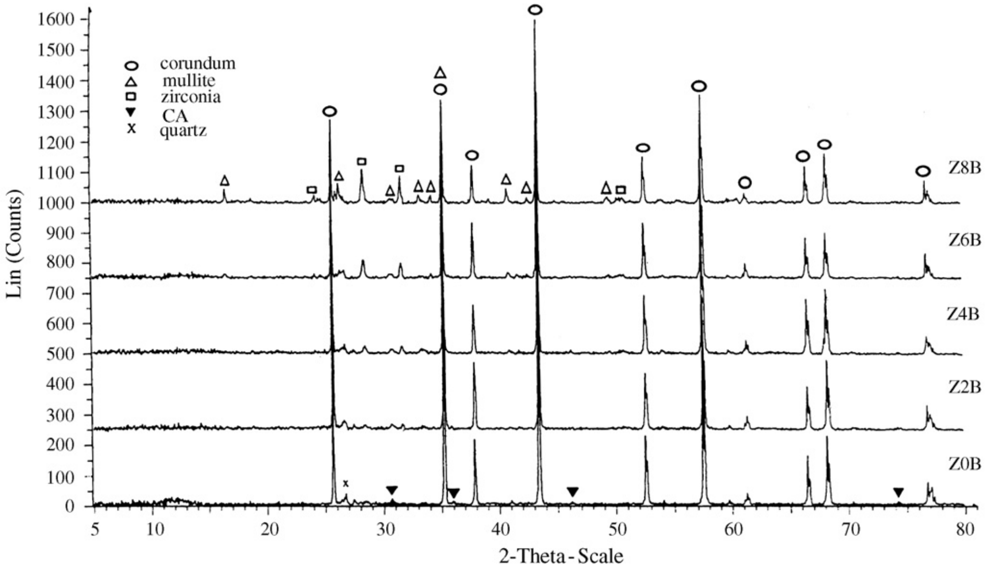

Fig. 2. XRD of fired bauxite castables at 1550 °C.

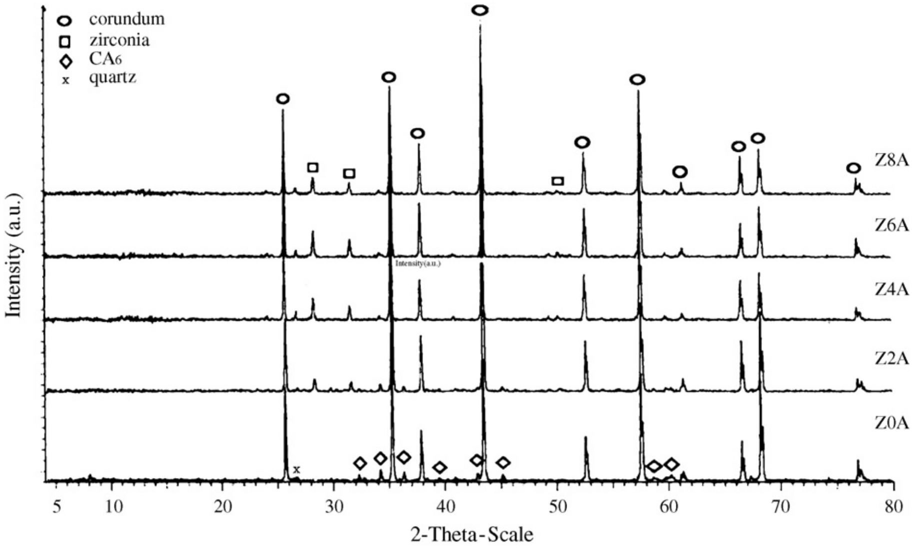

Fig. 3. XRD of fired alumina castables at 1550 °C.

alumina and bauxite), as we proceed from Z0 to Z8, the peak intensities of CA or CA_6 phases decreased. New phases of monoclinic zirconia (m-ZrO_2), mullite ($3Al_2O_3{\cdot}2SiO_2$) and quartz (SiO_2) were found in the series prepared from bauxite, while phases of monoclinic zirconia (m-ZrO_2) and quartz were detected in the series prepared from calcined alumina. This means that, after firing at 1550 °C, zircon is dissociated into m-ZrO_2 and SiO_2. Silica from zircon and silica present in bauxite as impurities reacts with fine alumina to form mullite. The presence of different impurities in bauxite versus alumina helps the densification process and the formation of mullite. The presence of quartz produced from the dissociation of zircon in alumina samples indicates that the firing temperature was insufficient for the sintering process.

3.2. Physico-mechanical properties

3.2.1. Water of consistency

Fig. 4 shows the water of consistency of the investigated castable samples prepared from pure alumina. The water addition to a castable has a significant and direct influence on the final properties and castable specifications. Excess water can reduce strength and increase shrinkage, while too little water can produce voids in the castable, causes poor consolidation and placement which will produce a weak porous concrete [32]. Fig. 4 shows a significant decrease in water consistency as cement content in the matrix decreases (which is the only cementing materials consuming water by hydration), i.e. from castable Z0A to Z8A. The water consistency of bauxite castables was similar to alumina castables.

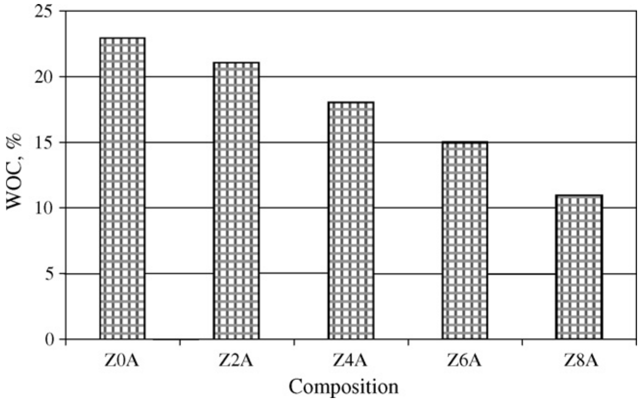

Fig. 4. Water consistency of alumina castables.

3.2.2. Bulk density and apparent porosity

The density and porosity ranges for the hydrated castables were in the range of 2.5–2.7 g/cm^3 and 20–30%, respectively, depending on the amount of high alumina cement, zircon and the type of aggregate. Fig. 5 shows densification parameter in terms of bulk density (BD) and apparent (AP) for both castables investigated after firing at 1550 °C. Generally, the densification parameters of castables obtained from bauxite aggregate are better than that obtained from pure alumina aggregate. This is due to the presence of some impurities in the bauxite aggregate which enhance the densification process by forming a liquid phase. As we go from Z0B to Z8B, an increase in bulk density and subsequently decrease in apparent porosity was obtained. This is attributed to the formation of mullite, which helps with

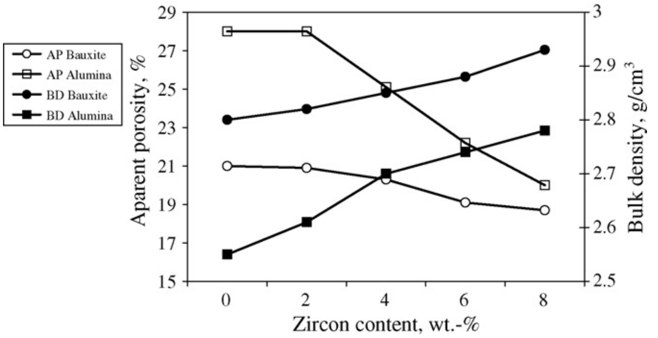

Fig. 5. Densification parameters of sintered castables.

the presence of a liquid phase that decreases the porosity and consequently increases the bulk density. On the other hand, castables prepared from pure alumina aggregate behave in the same trend, but with lower values. This is due to high purity alumina aggregate and the absence of a liquid phase.

Previous work [33] dealing with bauxite castables containing up to 8 wt.% SiC had a bulk density higher than that obtained in the present investigation. This may be due to the difference in particle size distribution of the aggregate used in that study.

3.2.3. Microstructure

The microstructural evolution of castables fired at 1550 °C was evaluated using the scanning electron microscope of representative regions of cut specimens. Figs. 6–8 show photomicrographs of castables prepared from alumina and bauxite aggregate after firing at 1550 °C for 2 h. The photomicrograph of Z0A castable in Fig. 6a exhibits a porous microstructure with rounded and well-defined edges alumina grains (point a). Hexagonal plate-like crystals (point b) were observed and identified as calcium hexa aluminate (CA_6) resulting from the reaction of CA and CA_2 phases with free alumina. On the other hand, photomicrographs of bauxite castables (Z0B; Fig. 6b and c) had a densely packed microstructure; with an abundant of corundum grains of comparable sizes (point a), embedded in the matrix. The matrix also has CA (point e) and some of liquid phase.

As we proceed from Z0B to Z8B as shown in Figs. 6–8, some needle-shaped mullite (point c) and rounded (ellipsoid) zirconia crystals (point d) are distributed from place to place, which reinforce the matrix and explained the high strength and refractory properties of the bauxite castables. The presence of such in situ formed mullite creates an interlocking microstructure in the bauxite castable castables. The Z4B sample (Fig. 7c and d) show locally agglomerated zirconia particles, but all other samples (Figs. 7a,b and 8a–d) exhibited well-distributed zirconia crystals. On the other hand, the impurities and high alumina cement present in the bauxite castables (especially higher content HAC batches) may form a low melting glass and tend to decrease the refractory properties. The structure of these samples appeared as partially diffused in some regions. The influence of trace impurities present during the processing of ceramics is well known and has been exploited in the control of densification, grain growth and morphology during sintering [34]. The ability to control microstructure is of central importance in achieving desired properties. The microstructure of the castables prepared from pure alumina was found to be relatively the same as that prepared using bauxite aggregate, but with higher porosity, well-defined grains and without a liquid phase in the matrix.

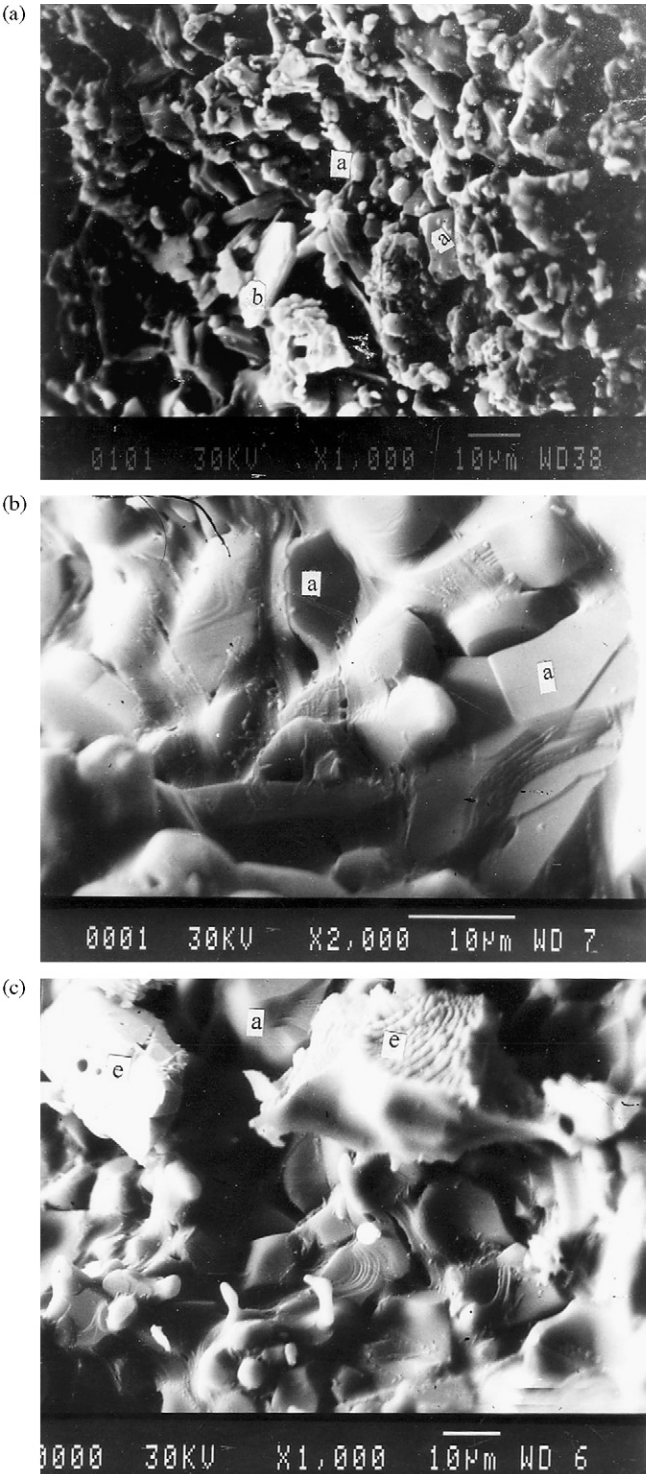

Fig. 6. SEM photomicrographs of (a) Z0A, and (b and c) Z0B castables fired at 1550 °C for 2 h.

3.3. Mechanical properties

Mechanical properties in terms of cold crushing strength of the hydrated (20 °C) and fired (1550 °C) castables (bauxite and alumina) are shown in Figs. 9 and 10. It can be seen that CCS of the hydrated specimens, i.e. green castables, decreases as the content of zircon increases at the expense of high alumina cement, which is responsible cold strength. It also appears that both hydrated castables have similar CCS after hydration. In both castable series, it appears that with increasing additions of zircon, the strength linearly deteriorates due to the decrease of cement content. Fired specimens show an improved CCS compared to the corresponding non-fired alumina and bauxite

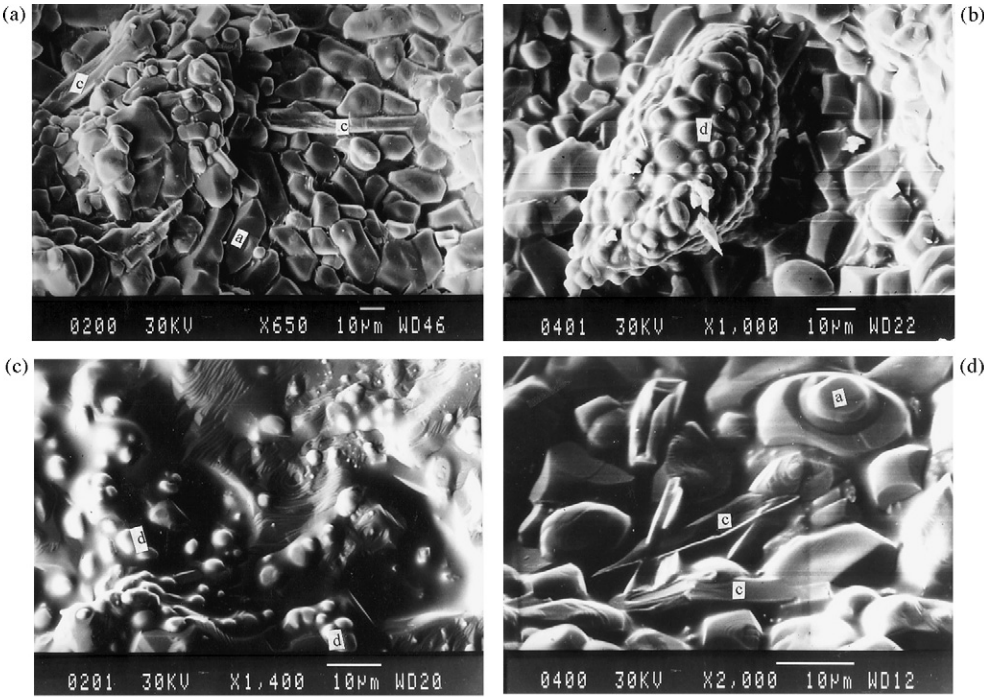

Fig. 7. SEM photomicrographs of Z2B (a and b) and Z4B (c and d) castables fired at 1550 °C for 2 h.

castables. This is due to the breakdown of weak hydraulic bonds and the formation of new strong ceramic bonds with increasing zircon content during firing at 1550 °C. In bauxite castables, the dissociation of zircon to m-ZrO_2 and SiO_2 helps in the formation of a composite material consisting of m-ZrO_2 and mullite ($3Al_2O_3{\cdot}2SiO_2$) due to the reaction of SiO_2 with fine alumina in the matrix. The presence of a m-ZrO_2–mullite composite in the matrix, which is characterized by high mechanical properties, is reflected on the strength of the whole castable sample. Figs. 9 and 10 show a great increase in strength of the fired samples as the contents of zircon increase. Generally, castables prepared from bauxite show higher CCS than those prepared using alumina aggregate. This is attributed to a higher content of impurities in the bauxite aggregate, which increases the liquid phase sintering and decreases the porosity, which consequently, tends to increase the room temperature

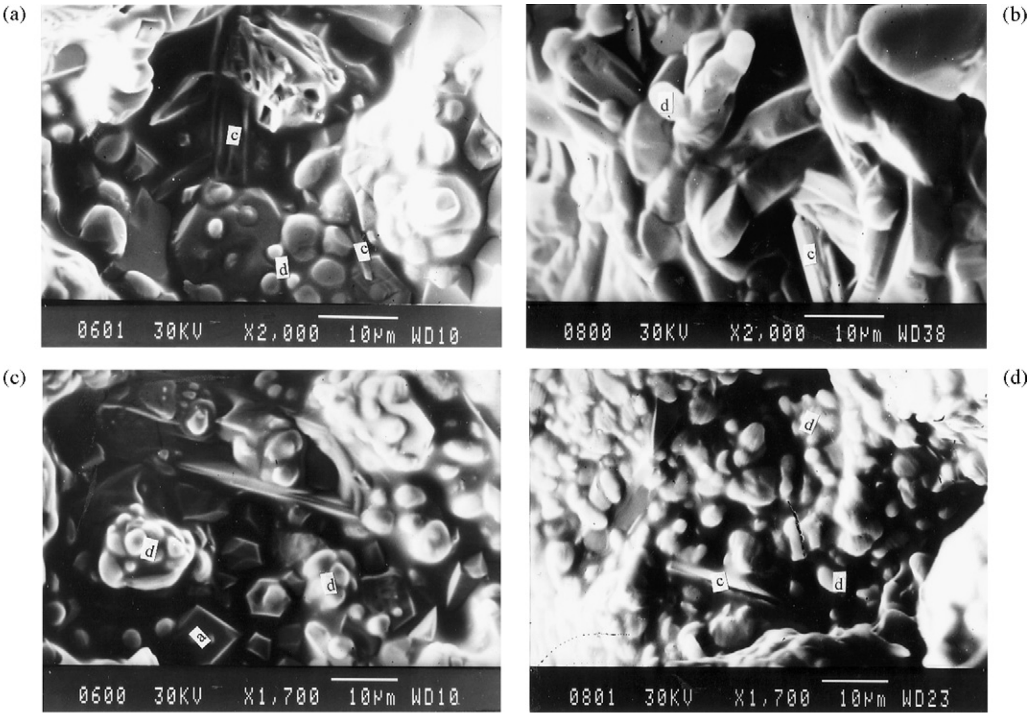

Fig. 8. SEM photomicrographs of Z6B (a and b) and Z8B (c and d) castables fired at 1550 °C for 2 h.

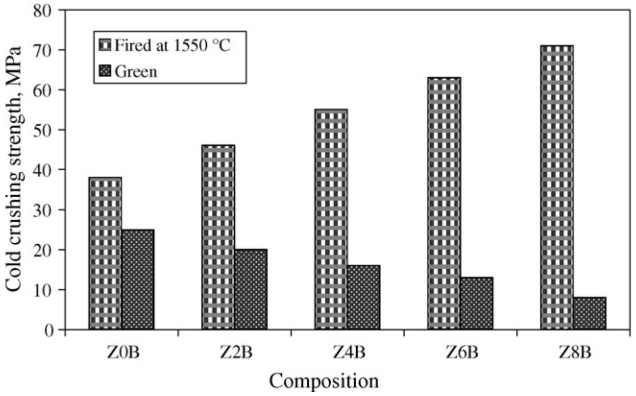

Fig. 9. Cold crushing strength of bauxite castables.

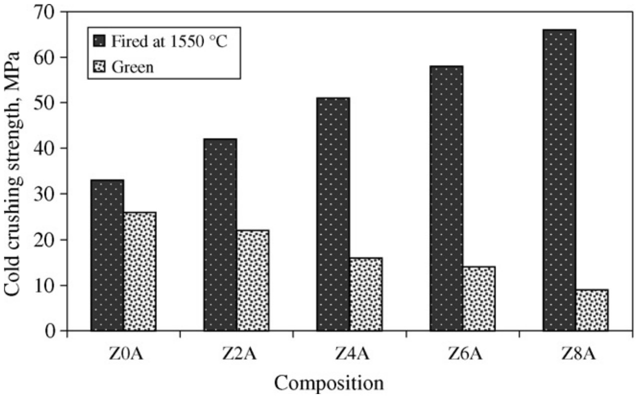

Fig. 10. Cold crushing strength of alumina castables.

mechanical properties. Also, the presence of a higher content of mullite (as indicated from XRD Fig. 2) in the castables prepared form bauxite rather than that prepared from alumina, improves the mechanical properties of that castables at that firing temperature. Alumina castables need a higher temperature for sintering to give higher CCS.

3.4. Refractory properties

3.4.1. Refractoriness under load and permanent linear change

Table 3 summarizes the refractory properties of both sintered refractory castables. Refractoriness under load (RUL) results are expressed in terms of T_0 and $T_{0.5}$, i.e. temperatures corresponding to the maximum expansion and 0.5% subsidence, respectively. These data confirm the improved loadbearing capacity of fired castables with decreasing HAC cement and increasing m-ZrO_2–mullite–corundum or m-ZrO_2–corundum composite in the matrix of (Z0B and Z0A), (Z4B and Z4A) and (Z8B and Z8A) samples. T_0 gradually increases from 1400–1450 °C to 1500–1550 °C in both castable series. Simultaneously, $T_{0.5}$ rises form 1500 and 1550 to >1550 and >1600 °C as we going from zero to 8% zircon additions in the bauxite and alumina castables. This is certainly a result of enhanced m-ZrO_2–mullite or m-ZrO_2–corundum formation, as confirmed by the investigation of phase composition and microstructure of the fired samples. The castables prepared from alumina aggregate show higher loadbearing capacity than that prepared from bauxite aggregate due to the higher purity of these castable and the formation of new refractory phase (CA_6) which also improve the high temperature refractory properties.

The high loadbearing capacity of the bauxite castable forming zirconia–mullite composites is supported by their volume stability, i.e. limited permanent linear change (PLC) when firing for 2 h at 1500 °C; as well as high thermal shock (TSR), as illustrated also in Table 3. All castables show less than 1.0% contraction after firing for 2 h at 1500 °C and survived more than 10 cycles of successive sudden cooling for 10 min in air.

3.5. Thermal shock resistance (TSR)

3.5.1. Residual strength ratio at $\Delta T = 1000$ °C

The thermal shock resistance properties are influenced by prefiring conditions and determined on specimens heated to a predetermined temperature (T), then quenched in air (T_{air}). After air cooling, the residual cold crushing strength (CCS_r) is measured and compared to the original strength (CCS_o). A residual strength ratio (CCS_r/CCS_o) at temperature difference $\Delta T = T - T_{\mathrm{air}}$ is the criterion for evaluating TSR.

The residual cold crushing strength ratio at $\Delta T = 1000$ °C of the alumina and bauxite castables was determined by measuring CCS before and after thermal shock cycling. The results shown in Fig. 11 demonstrate that the residual strength ratio of zircon-containing castables is increased with increasing zircon content. The maximum strength is attained in castables with 8 wt.% zircon.

Table 3
Refractory properties of prepared castables

Zircon content (wt.%)	TSR (cycle)		CCS (MPa)				PLC (2 h, 1500 °C)	RUL (°C)			
	Bauxite castable	Alumina castable	Before TSR test		After TSR test			Bauxite castable		Alumina castable	
			Bauxite	Alumina	Bauxite	Alumina		T_0	$T_{0.5}$	T_0	$T_{0.5}$
0	>10	>10	38	33	23	18	<1	1400	1500	1450	>1550
2	>10	>10	46	42	31	25	<1	–	–	–	–
4	>10	>10	55	51	43	33	<1	1430	1550	1500	>1550
6	>10	>10	63	58	55	46	<1	–	–	–	–
8	>10	>10	71	66	65	57	<1	1500	>1550	>1550	>1600

TSR: thermal shock resistance; CCS: cold crushing strength; PLC: permanent linear change; RUL: refractoriness under load.

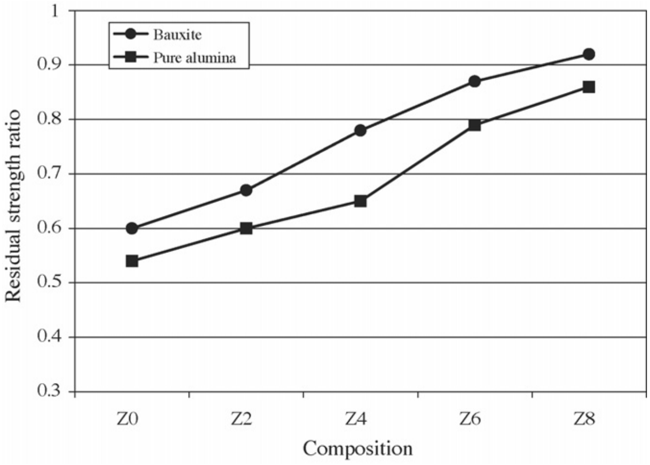

Fig. 11. Residual strength ration of sintered castables.

3.5.2. *Critical temperature difference* (ΔT_c)

The samples (Z6B and Z8B) and (Z6A and Z8A) were selected for determining changes in cold crushing strength after thermal shock for ΔT from 0.00 to 1300 °C. As seen from Fig. 12, there was no change in strength for either the bauxite and alumina castables up to about 850 °C; however, at higher temperatures, the strength decreased considerably. It is concluded that the critical temperature difference (ΔT_c) for both specimens is approximately 800–900 °C. According to Hasselman theory [35], ΔT_c indicates the ability of material to withstand abrupt temperature variations. In this case, when ΔT is from RT to 900 °C, the interior of the castables is not affected by thermal shock, and remains intact. Whereas when ΔT is in the range of 900–1300 °C, the castable is affected by thermal shock as the high thermal stresses generated in the material extend existing cracks and initiate new cracks, leading to lower strength. The improvement of TSR in these castable through zircon additions may be due to the higher thermal conductivity, lower thermal expansion, or the higher strength of m-ZrO_2–mullite composite, as well as to the presence of prismatic and elongated grains in the microstructure of alumina and bauxite castables. The formation of those crystals in castable matrices produce reinforced, but flexible structures; which lead to an increase in the strength and spalling resistance. The castables-containing no zircon showed the same trend but with lower values.

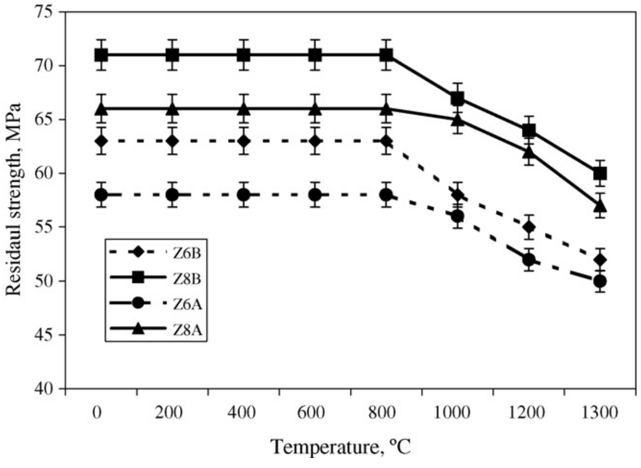

Fig. 12. Critical temperature difference of Z6B and Z6A castables.

4. Conclusion

Castables containing bauxite aggregate showed higher densities and room temperature mechanical properties due to the presence of impurities in the bauxite aggregate. These impurities helped liquid phase sintering, and consequently improved the mechanical properties. In contrast, castables containing pure alumina aggregate exhibited higher refractory properties due to greater aggregate purity and the presence of a CA_6 phase. The emergence of refractory phases such as mullite and zirconia or CA_6 was observed to have beneficial effects on mechanical and refractory properties due to the development of morphologies, which interlocked other phases, and due to pore filling from expansible reactions.

References

[1] S. Ghosh, R. Majumdar, B.K. Sinhamahapatra, R.N. Nandy, M. Mukherjee, S. Mkhopadhyay, Microstructure of refractory castables prepared with sol–gel additives, Ceram. Int. 29 (2003) 671–677.

[2] R. Myhre, Hot strength and bond phase reaction in low and ultra low cement castable, in: UNITECR, 93 Congress, Sao Paulo, Brazil, (1993), pp. 583–594.

[3] M.D.M. Innocentini, R.F. Pardo, V.C. Pandolfeli, Influence of air compressibility on the permeability of refractory castables, J. Am. Ceram. Soc. 83 (2000) 1536–1538.

[4] Z. Li, G. Ye, Bonding and recent progress of monolithic refractories, Interceram 41 (3) (1992) 169–172.

[5] F.N. Cunha, R.C. Bradt, Reactions of constituents for in situ bonds of $MgAl_2O_3$, Mg_2SiO_4 and $3Al_2O_3$ $2SiO_2$, in: Refractories, 57th Electric Furnace Conference, Pittsburgh, PA, USA, (1999), pp. 143–152.

[6] B. Sandberg, B. Myhre, J.L. Holm, Castables in the system $MgO–Al_2O_3–SiO_2$, in: UNITECR 95, vol. 2, Kyoto, Japan, (1995), pp. 173–180.

[7] F. Azizian, Development of no cement castables, Refractories Appl. 2 (1996) 6–7.

[8] A.L. Gentile, W.R. Foster, Calcium hexa-aluminate and stability relations in the system $CaO–Al_2O_3–SiO_2$, J. Am. Ceram. Soc. 46 (1994) 274–276.

[9] F. Ye, M. Rigaud, X. Liu, X. Zhong, High temperature mechanical properties of bauxite-based SiC-containing castables, Ceram. Int. (2004).

[10] M.F. Zawrah, N.M. Khalil, Effect of mullite formation on properties of refractory castables, Ceram. Int. 27 (2001) 689–694.

[11] B. Clavaud, J.P. Radal, A new generation of low-cement castables, in: R.E. Fisher (Ed.), Advances in Ceramics, Vol. 13, New Development in Monolithic Refractories, American Ceramic Society, Columbus, OH, 1985, pp. 274–282.

[12] L. Prost, A. Pnillac, Hydraulically setting refractory compositions, Fr. Pat. No. 6934405, 1969.

[13] B. Myhre, Strength developments of bauxite-based ultra low cement castables, Am. Ceram. Soc. Bull. 73 (5) (1994) 68–73.

[14] U. Schumaher, Untersuchungen an Zementarmen und Ultrafalishen Korundfeuerbetones, Ph.D. thesis, Rheinisch-Westfalishen Technishen Hohschule, Aachen, FRG, 1988.

[15] A. Mathieu, A. Campas, J. Bayoux, D. Richon, Calcium aluminate cement and reactive alumina, in: UNITECR'93 Congress, Sao Paulo, Brazil, pp. 672–682.

[16] B. Myhre, Hot strength and bond-phase reactions in low and ultra-low cement castables, in: UNITECR'93 Congress, Sao Paulo, Brazil, pp. 583–594.

[17] L. Zaigeng, Z. Luning, Y. Guotian, Z. Ninheng The effect of some ultra fine oxides on the properties of ultra low cement corundum based castables, in: Proceedings of the 35th International Colloquium on Refractories, Aachen, 1992.

[18] G. Maczura, J. Kopanda, F. Rohr, Calcium aluminate cements for emerging castable technology, in: R.E. Fisher (Ed.), Advances in Ceramics, Vol. 13, New Development in Monolithic Refractories, American Ceramic Society, Columbus, OH, 1985, pp. 285–304.

[19] A. Hundere, B. Myhre, On the influence of superfines in high-alumina castables, in: Proceedings of the 39th International Colloquium on Refractories, Aachen, 1996.

[20] A. Hundere, B. Myhre, Effect of different finest fractions (SiO_2 and/or Al_2O_3) in alumina based ultra low cement castables, in: Proceedings of the American Ceramic Society 98th Annual Meeting, Indianapolis, 14–17 April 1996.

[21] B. Sandberg, B. Myhre, J.L. Holm, Castables in the system $MgO–Al_2O_3–SiO_2$, UNTECR'95, Kyoto, Japan, 19–23 November 1993.

[22] B. Myhre, Microsilica in alumina based ultra low cement castables; the effect of microsilica addition on flow, in: Proceedings of the 23rd ALAFAR Congress in Puerto Vallara, Mexico, 6–10 November 1994.

[23] B. Myhre, Ultra low cement; casting and set properties of secar cements with additives, in: Proceedings of the 20th ALAFAR Congress, Chile, 1990.

[24] B. Myhre Cement free castables in the system $MgO–SiO_2$; the effect of bond phase modifier on strength, in: proceedings of the American Ceramic Society, 93rd Annual Meeting in Cincinnati, Ohio, 15 May 1991.

[25] YuE. Piviniski, New refractory concrete and bonding systems, Refract. Ind. Ceram. 39 (314) (1998) 91–99.

[26] W. Kronert, U. Schumacher, Use of low-cement and ultra low cement refractory castables in iron and steel industry furnace prospect, Interceram (Aachen Proc. 1988) 3 (8) (1989) 12–18.

[27] R.E. Fisher, in: Proceedings of the 28th Annual Symposium on Refractories, American Ceramic Society, Columbus, OH, 1992.

[28] K. Shaw, Refractories and Their Uses, Applied Science Publisher, London, 1972.

[29] J.H. Chester, Refractories Production and Properties, Iron and Steel Institute, London, 1973.

[30] S.C. Carnglia, G.L. Barna, Hand Book of Industrial Refractories Technology, Noyes Publications, Park Ridge, NJ, 1992.

[31] G. Routschka (Ed.), Pocket Manual on Refractories, Vulkan Verlag, Essen, 1997.

[32] R. Stieling, H.-J. Kunkel, U. Martin, Vibrated castables with a thixotropic behavior, in: R.E. Fisher (Ed.), Advances in Ceramics, Vol. 13; New Development in Monolithic Refractories, American Ceramic Society, Columbus, OH, 1995, pp. 211–218.

[33] M.F. Zawrah, N.M. Khalil, High-alumina castables reinforced with SiC, Adv. Appl. Ceram. 104 (6) (2005) 312–317.

[34] S.J. Bennison, M.P. Harmer, in: C.A. Handwerker, J.E. Blendell, W.A. Kaisser (Eds.), Ceramic Transactions, vol. 7, The American Ceramic Society, Westerville, OH, USA, 1990, p. 13.

[35] D.P.H. Hasselman, in: W.W. Kriegel, H. Palmour, III (Eds.), Ceramics in Severe Environments, Plenum Press, New York, 1971, pp. 89–101.